A Novel Non-Reciprocal Surface Acoustic Wave Filter

Jose Antonio Bahaonde[#1], Ioannis Kymissis[#2],
[#]Columbia University, USA
[1]jab2361@columbia.edu, [2]johnkym@ee.columbia.edu

***Abstract*— Limit your abstract to one paragraph and keep it short. In the Keywords section, include a few keywords from: http://www.ieee.org/organizations/pubs/ani_prod/keywrd98.txt**

***Keywords*— ceramics, coaxial resonators, delay filters, delay lines, power amplifiers.**

I. Introduction

Acoustic devices have played a major role in telecommunications for decades as the leading technology for filtering in RF and microwave frequencies. While filter requirements for insertion loss and bandwidth become more stringent, more functionality is desired for many applications to improve overall system level performance. For instance, a filter with non-reciprocal transmission can minimize losses due to mismatch and protect the source from reflections while also performing its filtering duties. A device such as this one was originally researched by scientists decades ago. These devices were based on the acoustoelectric effect where surface acoustic waves (SAW) traveling in the same direction are as drift carriers in a nearby semiconductor are amplified. While several experiments were successfully demonstrated in [1], [2], [3]. these devices suffered from extremely high operating electric fields and noise figure [4], [5].

In the past few years, new techniques have been developed for implementing non-reciprocal devices such as isolators and circulators without utilizing magnetic materials [6], [7], [8], [9]. The most popular technique has been spatio-temporal modulation (STM) where commutated clock signals synchronized with delay elements result in non-reciprocal transmission through the network. STM has also been adapted by researchers to create non-reciprocal filters. The work in [10] utilizes 4 clocks signals to obtain a non-reciprocal filter with an insertion loss of -6.6 dB an isolation of 25.4 dB. Another filter demonstrated in [11] utilizes 6 synchronized clock signals to obtain a non-reciprocal filter with an insertion loss of -5.6 dB and an Isolation of 20 dB.

In this work, a novel non-reciprocal topology is explored with the use of only one modulation signal. The design is based on asymmetrical SAW delay lines with a parametric amplifier. The device can operate in two different modes: phase coherent mode and phase incoherent mode. In phase coherent mode, the device is capable of over +12 dB of gain and 20.2 dB of isolation. A unique feature of this mode is that the phase of the pump signal can be utilized to tune the frequency response of the filter. Under the phase-incoherent mode, the pump frequency remains constant and the device behaves as a normal filter with non-reciprocal transmission exhibiting over +7 dB of gain and 17.33 dB of isolation. While the tuning capability is lost in this mode, phase-coherence is no longer necessary so the device can be utilized in most filtering applications.

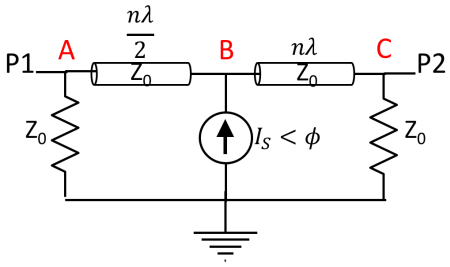

Fig. 1. Network of two asymmetrical transmission lines surrounding a current source.

II. A Non-Reciprocal Topology based on Asymmetrical Transmission Lines

Fig. 1 illustrates the two-port network the device is based on. While simplistic, it is effective in providing insight how non-reciprocity can be achieved. The structure is based on two 50Ω transmission lines of lengths $\frac{\lambda}{2}$ and λ where λ is the wavelength. Between the transmission lines is a current source of magnitude I_S and phase ϕ. It also holds the property that its frequency is exactly that of the input signals coming in ports P1 and P2. Using these definitions, the forward and reverse s-parameters, S_{21} and S_{12} can be derived using conventional microwave analysis techniques. If a test signal of magnitude V_{IN} and a phase of θ is applied to P1, the forward and reverse S-parameters can be written as

$$S_{21} = \frac{-2\left(2V_{IN}e^{-j\theta} - Z_0 I_S e^{-j(\phi+\beta L_1)} + 3Z_0 I_S e^{j(\beta L_2-\phi)}\right.}{V_{IN}e^{-j\beta(L_1+L2)} - 9e^{j\beta(L_1+L2)}}. \tag{1}$$

and

$$S_{12} = \frac{-2\left(2V_{IN}e^{-j\theta} - Z_0 I_S e^{-j(\phi+\beta L_2)} + 3Z_0 I_S e^{j(\beta L_1-\phi)}\right.}{V_{IN}e^{-j\beta(L_1+L2)} - 9e^{j\beta(L_1+L2)}}. \tag{2}$$

If the transmission lines lengths from Fig. 1 are considered and $\theta = \phi = 0°$, 1 and 2 become

$$S_{21} = \frac{-(4V_{IN} + 16Z_0 I_S)}{9V_{IN}} \tag{3}$$

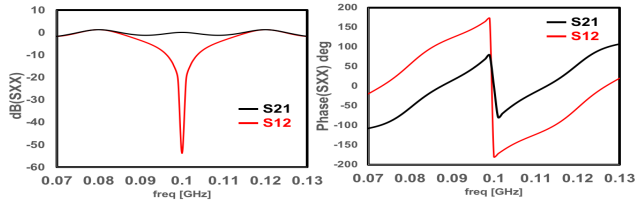

Fig. 2. Magnitude (left) and phase (right) of forward and reverse s-parameters for the condition $I_S \simeq \frac{V_{IN}}{4Z_0}$ and $\theta = \phi = 0°$.

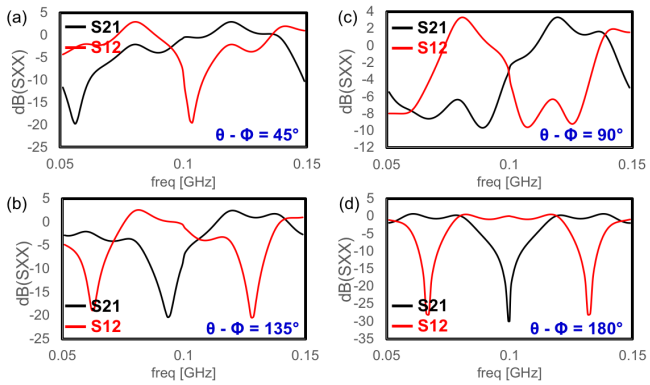

Fig. 3. Magnitude of forward and reverse s-parameters for the condition $I_S \simeq \frac{V_{IN}}{4Z_0}$ at different phase relationships: (a) $\theta = \phi = 45°$ (b) $\theta = \phi = 90°$, (c) $\theta = \phi = 135°$, and (d) $\theta = \phi = 180°$.

and

$$S_{12} = \frac{-(4V_{IN} - 16Z_0 I_S)}{9V_{IN}}. \tag{4}$$

Upon visual inspection of 3 and 4, due to the sign flip caused by the terms $e^{-j(\beta L_1)} = -1$ and $e^{-j(\beta L_2)} = 1$, the contribution of the current source gets added in the forward direction and subtracted in the reverse direction. If $I_S \simeq \frac{V_{IN}}{4Z_0}$, as seen in Fig. 2, the frequency response is that of an isolator where the signal is transmitted in the forward direction and attenuated in the reverse direction. An interesting feature of this topology is that if the phase relationship between the input signal and current source is controlled, the frequency response and non-reciprocal behavior can be changed. As seen in Fig. 3, the point of maximum isolation changes as the phase difference changes from $45°$ to $135°$ (Fig. 3 (a)-(c)). Furthermore, the isolation behavior occurs in both directions at different frequencies resulting in a non-reciprocal duplexing action. When the phase difference reaches $180°$ the isolation behavior around the center frequency is reversed.

If the current source is now tuned so that $I_S >> \frac{V_{IN}}{4Z_0}$, the contribution of the current source dominates the numerator resulting in the frequency response shown in Fig. 4. Under this condition, the non-reciprocity is weak, however, at the center frequency, there exist is a $180°$ phase difference between forward and reverse signals. This can be leveraged to create non-reciprocity without the need of phase-coherence between signals.

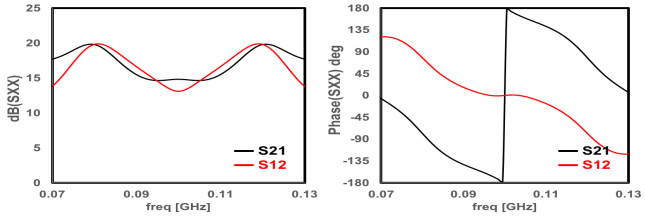

Fig. 4. Magnitude (left) and phase (right) of forward and reverse s-parameters for the condition $I_S >> \frac{V_{IN}}{4Z_0}$ and $\theta = \phi = 0°$.

A. The Current Source

As demonstrated in the previous section, the non-reciprocal behavior of the structure is a result of the transmission line lengths, but it is also dependent on a current source that is able to track the frequency of the incoming signal. This can be implemented with a degenerate parametric amplifier.

Parametric amplification is an RF to RF power conversion that occurs by pumping a varactor with a large signal at frequency f_P to amplify a small signal at frequency f_S. As discussed in [12], there exist several configurations and operating conditions by which parametric amplifiers can function. One configuration is known as the phase-coherent degenerate amplifier (PCDA) that occurs when $f_P = 2f_S$. Under this condition, the pump action results in negative resistance which amplifies the source signal. Since the mixing product lies on f_S, the total gain is maximized by controlling the phase of the pump signal so that both signal interfere constructively [13], [14]. The PCDA provides exactly the type of current source required for this application to demonstrate a non-reciprocal characteristics shown in Fig. 2 and Fig. 3.

While the PCDA produces the desired signal, this type of amplifier requires that the condition $f_P = 2f_S$ be satisfied and foreknowledge of the source signal phase. Since this is difficult to deploy in practical system, it is desirable to asses functionality in a phase-incoherent mode. In degenerate parametric amplifiers this occurs when $f_P \neq 2f_S$, thus, the idler signal appears at $f_P - f_S$. The choice of f_P is made so that f_i exist within the same bandwidth of f_S or outside of it, requiring it's own termination circuitry. Both signals at f_S and f_i are amplified, but the phase the phase of the signal at f_S is unaffected by the pump phase. The lost of phase of control signifies that the device can no longer be operated in a phase-coherent manner. This is analogous to the case where $I_S >> \frac{V_{IN}}{4Z_0}$ in Fig. 4 which will result in weak non-reciprocity.

B. Asymmetrical Power Division Via Uni-directional SAW Transducers

The loss of isolation in the structure is due to the signal from the parametric amplifier dominating the incoming signal. If node B in Fig. 1 was able to distribute the power from the amplifier asymmetrically, the strong non-reciprocal behavior could be regained. This can be achieved in the acoustic domain utilizing uni-directional SAW transducers.

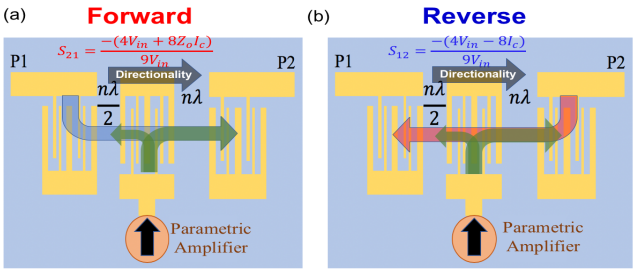

Fig. 5. (a) Forward direction with test signal applied at P1. A fraction of the signal is absorbed and is reflected back with gain where it constructively interferes with source signal at P2. (b) Reverse direction where test signal is applied at P2. The signal is absorbed and reflected back with gain to P2. A fraction of the amplified version destructively interferes with the source signal at P1.

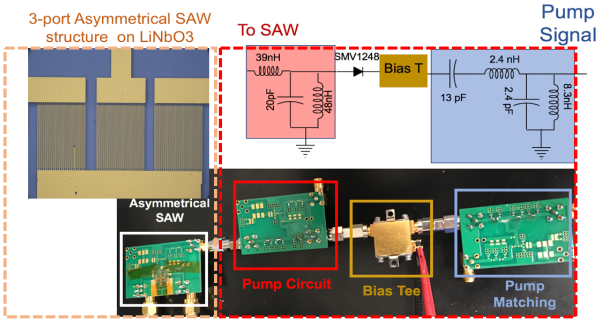

Fig. 6. Schematic and prototype of the non-reciprocal SAW Filter. All components except the SAW device are off the shelf surface mount devices.

The structure in Fig. 1 can be implemented in the acoustic domain by placing the transducers in node A, B, and C. This has the added advantaged of miniaturizing the device that would otherwise be very large in the electromagnetic domain. Furthermore, the center transducer at node B can be implemented with a uni-directional transducer. The conventional SAW transducer is bi-directional and emits acoustic energy in both directions equally. A uni-directional transducer can be designed to favor one direction so that the power is divided asymmetrically to P1 and P2. Fig. 5 (a) and (b) demonstrates how this device behaves with a center transducer with directionality to the right. In the forward direction, (Fig. 5 (a)), a fraction of the input signal in blue is absorbed by the center transducer where it becomes amplified by the parametric amplifier and adds in phase with the input signal arriving at P2. The reverse direction is shown in Fig. 5 (b) where the incoming signal in red is absorbed by the center transducer where it becomes amplified and is then emitted by the center transducer with most of the signal being diverted to opposite direction. The signal then destructively interferes at with the input signal at P1.

III. Design

Fig. 6 shows the schematic and prototype of the device. The pump circuit, highlighted in red, is composed of three sections: the pump match circuit, the bias-T and varactor, and

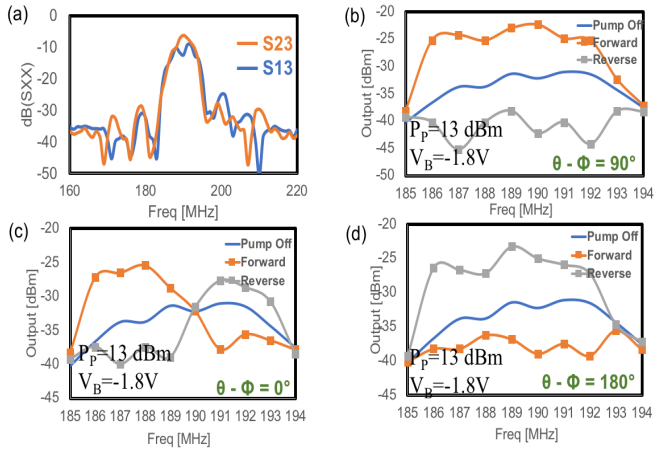

Fig. 7. (a) Transmission S-parameters of center transducer to input and output transducers. (b) Forward and reverse transmission for $\phi - \theta = 0°$. (c) Forward and reverse transmission for $\phi - \theta = 90°$. (d) Forward and reverse transmission for $\phi - \theta = 180°$. All measurements are done with P_P= 13 dBm and $V_B = -1.8V$.

the pump circuit. The pump circuit is a 2nd order resonant network that resonates out the capacitance of the center transducer at the upper and lower band edges of the SAW filter. A skyworks hyper-abrupt junction diode with part number SMV1248 is used as the varactor with an SMA bias-T to reverse bias the diode. The pump match network is a 2nd order high-pass network which matches the impedance of the rest of the circuit to a 50Ω pump source. The cut-off frequencies of both the pump circuit and pump match circuits provide additional isolation between the source and pump signals. The SAW structure was fabricated on 128° Y-cut $LiNbO_3$. The device was designed according to [15] with a center frequency of 190 MHz. The center transducer is offset from $\frac{\lambda}{2}$ to obtain the required asymmetry. Fig. 7 (a) demonstrates the transmission from the center transducer (Port 3) to the transducer to the left (Port 1) and to the right (Port2). As seen here, there is a 5 dB difference in transmission. The input and output transducers are also uni-directional to minimize bi-directional loss.

IV. Results

A. Phase-Coherent Mode

The phase coherent mode is measured by utilizing two signal generators synchronized to their 10 MHz clock reference. One signal generator (SG) behaves a small signal source and the other as the pump source. The output of the device is connected to a spectrum analyzer (SA) to measure the output power. The measurement is carried out by first setting the SG frequencies so that $f_P = 2f_S$ and then adjusting the phase of the pump SG to obtain the desired phase relationship. Once this is accomplished, the data from the SA is recorded and the measurement is repeated at a different frequency. Fig. 7 (a) shows the output power for phase difference $\phi - \theta = 0°$ when the pump is off, on, and on with input and output connections reversed. The device demonstrates a gain of up

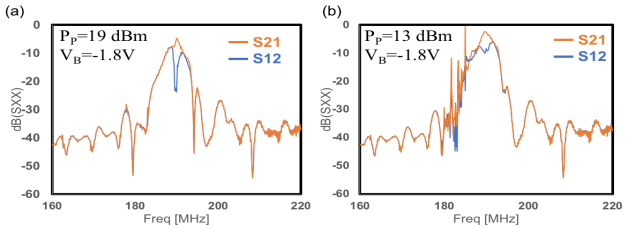

Fig. 8. (a) Forward and reverse s-parameters for f_P = 366 MHz, P_P=19 dBm, and V_B = -1.8V. (b) Forward and reverse s-parameters for f_P = 366 MHz, P_P=13 dBm, and V_B = -1.8V.

to +12 dB throughout the 8 MHz bandwidth of the device. In the reverse direction, the signal is attenuated by up to 8 dB obtaining a maximum isolation of 20.2 dB. When the phase difference is $\phi - \theta = 90°$, Fig. 7 (c), the response mimics as in theory where there exist a duplexing action in forward and reverse signals. As expected, the uni-directionality is reversed when the phase difference is $\phi - \theta = 180°$, Fig. 7 (d).

B. *Phase-Incoherent Mode*

Since this mode does not require foreknowledge of the phase of the input signal, the measurement is carried out with a network analyzer connected to P1 and P2 and a signal generator providing the pump signal. In this case, the pump frequency is kept constant. Fig.8 (a) shows the measured forward and reverse s-parameters for f_P=366 MHz at a power of 19 dBm. The device demonstrates +7dB of gain and on isolation of 17.36 dB. It is important to note that in this case, the idler signal is not supported by the SAW or any peripheral circuitry. This causes the required pump power to increase. In contract, if f_P=375 MHz, the idler is supported by the SAW and thus a lower power is required to obtain the results in Fig.8 (b). Due to this, more gain is available showing an improvement of up to +10 dB with a pump power of 13 dBm. The isolation obtained in this case is 7.2 dB. The non-reciprocity is also observed over a wider bandwidth when the idler is appropriately supported.

V. Conclusion

Table 1 compares the results obtained with the device presented here with the state-of-the-art. The device compares favorably in both insertion loss and isolation when compared to non-reciprocal filters utilizing STM. While the highest gain and isolation are achieved in the phase-coherent mode, this comes at the cost of the required circuitry to implement obtain phase coherence. The phase-incoherent mode is does not require phase information so it is readily applicable to most filtering applications. Further work is currently underway to characterize the noise and linearity of the device as well as other modes of operation utilizing a non-degenerate amplifier.

Table 1. Comparison with state-of-the-art work in non-reciprocal acoustic devices.

Works	IL [dB]	Isolation [dB]	f_0 [MHz]	# of LOs
[16] (2019)	-60	16	252	0
[10] (2018)	-6.6	25.4	155	4
[11] (2018)	-5.6	15	1000	6
[9] (2018)	-2.8	12	172	4
This work	-5.6/-3.2	7.2/20.2	189	1

Acknowledgment

This work was supported by the Nation Science Foundation (NSF) Emerging Frontiers in Innovation and Research (EFRI) program 1641100. We would also like to thank Harish Krishnaswamy for his support and supplying measurement facilities.

References

[1] J. H. Collins, K. M. Lakin, C. F. Quate, and H. J. Shaw, "Amplification of acoustic surface waves with adjacent semiconductor and piezoelectric crystals," *Applied Physics Letters*, vol. 13, no. 9, pp. 314–316, 1968. [Online]. Available: https://doi.org/10.1063/1.1652628

[2] L. A. Coldren and G. S. Kino, "Monolithic acoustic surface-wave amplifier," *Applied Physics Letters*, vol. 18, no. 8, pp. 317–319, 1971. [Online]. Available: https://doi.org/10.1063/1.1653677

[3] K. Yamanouchi and K. Shibayama, "Propagation and amplification of rayleigh waves and piezoelectric leaky surface waves in linbo3," *Journal of Applied Physics*, vol. 43, no. 3, pp. 856–862, 1972.

[4] G. Kino and L. Coldren, "Noise figure calculation for the rayleigh wave amplifier," *Applied Physics Letters*, vol. 22, no. 1, pp. 50–52, 1973. [Online]. Available: https://doi.org/10.1063/1.1654471

[5] G. S. Kino, "Acoustoelectric interactions in acoustic-surface-wave devices," *Proceedings of the IEEE*, vol. 64, no. 5, pp. 724–748, May 1976.

[6] N. Reiskarimian and H. Krishnaswamy, "Magnetic-free non-reciprocity based on staggered commutation," *Nature Communications*, vol. 7, p. 11217, 2016. [Online]. Available: http://www.nature.com/doifinder/10.1038/ncomms11217

[7] N. A. Estep, D. L. Sounas, and A. Alu, "Magnetless microwave circulators based on spatiotemporally modulated rings of coupled resonators," *IEEE Transactions on Microwave Theory and Techniques*, vol. 64, no. 2, pp. 502–518, 2016.

[8] T. Dinc and H. Krishnaswamy, "A 28ghz magnetic-free non-reciprocal passive cmos circulator based on spatio-temporal conductance modulation," *Digest of Technical Papers - IEEE International Solid-State Circuits Conference*, vol. 60, pp. 294–295, 2017.

[9] J. Bahamonde, I. Kymisis, A. Alu, and H. Krishnaswamy, "1.95-ghz circulator based on a time-modulated electro-acoustic gyrator," in *Proc. IEEE Int. Symp. Antennas and Propagation and USNC-URSI Radio Science Meeting*, July 2018.

[10] R. Lu, T. Manzaneque, Y. Yang, A. Gao, L. Gao, and S. Gong, "A radio frequency non-reciprocal network based on switched low-loss acoustic delay lines," Oct 2018, pp. 1–4.

[11] M. Pirro, C. Cassella, G. Michetti, G. Chen, P. Kulik, Y. Yu, and M. Rinaldi, "Novel topology for a non-reciprocal mems filter," in *2018 IEEE International Ultrasonics Symposium (IUS)*, Oct 2018, pp. 1–3.

[12] J. M. Manley and H. E. Rowe, "Some general properties of nonlinear elements-part i. general energy relations," *Proceedings of the IRE*, vol. 44, no. 7, pp. 904–913, July 1956.

[13] L. Blackwell and K. Kotzebue, *Semiconductor-Diode Parametric Amplifiers*, 1961.

[14] E. D. Reed, "The variable-capacitance parametric amplifier," *IRE Transactions on Electron Devices*, vol. 6, no. 2, pp. 216–224, April 1959.

[15] T. Thorvaldsson, "Analysis of the natural single phase unidirectional saw transducer," in *Proceedings., IEEE Ultrasonics Symposium,*, Oct 1989, pp. 91–96 vol.1.

[16] M. Ghatge, G. Walters, T. Nishida, and R. Tabrizian, "A non-reciprocal filter using asymmetrically transduced micro-acoustic resonators," *IEEE Electron Device Letters*, vol. 40, no. 5, pp. 800–803, May 2019.